


# High mRNA expression of POU2F3 in small cell lung cancer cell lines predicts the effect of lurbinectedin

Shinji Matsui<sup>1</sup> | Tomohiro Haruki<sup>1</sup>  | Yuki Oshima<sup>1</sup> | Yoshiteru Kidokoro<sup>1</sup> | Tomohiko Sakabe<sup>2</sup> | Yoshihisa Umekita<sup>2</sup> | Hiroshige Nakamura<sup>1</sup>

<sup>1</sup>Department of Surgery, Division of General Thoracic Surgery, Faculty of Medicine, Tottori University, Tottori, Japan

<sup>2</sup>Department of Pathology, Division of Pathology, Faculty of Medicine, Tottori University, Tottori, Japan

## Correspondence

Tomohiro Haruki, Department of Surgery, Division of General Thoracic Surgery, Faculty of Medicine, Tottori University, 36-1 Nishi-cho, Yonago, Tottori 683-8504, Japan.  
Email: tomohiroh@tottori-u.ac.jp

## Funding information

Japan Society for the Promotion of Science, Grant/Award Number: JP 19K18215

## Abstract

**Background:** Small cell lung cancer (SCLC) is a progressive disease with a poor prognosis. Recently, a method to classify SCLC by the expression status of four transcription factors, ASCL1, NEUROD1, POU2F3, and YAP1, was proposed. Here, we investigated the potential relationships between expression of these four transcription factors and the effect of lurbinectedin.

**Methods:** mRNA and protein expression of ASCL1, NEUROD1, POU2F3, and YAP1 were quantified in eight SCLC cell lines and analyzed for potential correlations with drug sensitivity. In addition, ASCL1, NEUROD1, POU2F3, and YAP1 expression were evaluated in 105 resected cases of high-grade neuroendocrine carcinoma of the lung, including 59 resected cases of SCLC.

**Results:** Based on the results of qRT-PCR and western blot analyses, the eight SCLC cell lines examined were classified into NEUROD1, POU2F3, and YAP1 subtypes, as well as five ASCL1 subtypes. There were no correlations between cell line subtype classification and drug sensitivity to cisplatin, etoposide, or lurbinectedin. Next, we compared relative mRNA expression levels of each transcription factor with drug sensitivity and found that the higher the mRNA expression level of POU2F3, the lower the IC<sub>50</sub> of lurbinectedin. Evaluation of resected SCLC tissue revealed that the composition of subtypes defined by the relative dominance of ASCL1, NEUROD1, POU2F3, and YAP1 was as follows: 61% ASCL1, 15% NEUROD1, 14% POU2F3, 5% YAP1, and 5% all-negative.

**Conclusion:** In our experiments, high mRNA expression of POU2F3 in SCLC cell lines correlated with the effect of lurbinectedin.

## KEYWORDS

small cell lung cancer, large cell neuroendocrine carcinoma, POU2F3, lurbinectedin

## INTRODUCTION

Lung cancer is the leading cause of cancer-associated mortality worldwide.<sup>1</sup> Approximately 15% of new lung cancer cases diagnosed each year are small cell lung cancer (SCLC).<sup>2,3</sup> Strongly associated with tobacco exposure and one of the most aggressive and recalcitrant cancers, SCLC is characterized by rapid growth with a short doubling time, early development of widespread metastasis, and a 5-year survival rate of less than 5%.<sup>4,5</sup> In terms of treatment, the efficacy of chemotherapy with

cisplatin plus etoposide for patients with SCLC was first demonstrated in 1979.<sup>6</sup> Since 1985, the etoposide-platinum-based doublet regimen has been the standard first-line systemic treatment for patients with extensive-stage SCLC<sup>7,8</sup>; indeed, this basic therapeutic approach has not changed for three decades. In contrast to non-small cell lung cancer, which shows remarkable improvement of survival with personalized treatment, SCLC has been treated as a single disease. Population-level mortality analysis in the United States (US) suggested that mortality from SCLC declined almost entirely as a result of

declining incidence, with no improvement in survival.<sup>1</sup> Although recent advances in immunotherapy have provided breakthroughs for the treatment of SCLC,<sup>2,3</sup> these options remain insufficient and survival outcomes have not been substantially extended.

In the past few years, much has been learned about SCLC through comprehensive genetic analysis and the establishment of genetically engineered mouse models and patient-derived xenografts.<sup>4,5</sup> Furthermore, the intratumoral heterogeneity of SCLC, often reported as “classic” and “variant” in cell line studies, has recently been proposed to be classifiable into four transcriptional subtypes: ASCL1, NEUROD1, POU2F3, and YAP1.<sup>6</sup> Time-series single-cell transcriptome analysis showed that MYC-driven subtypes changed from ASCL1 to NEUROD1 to YAP1 over time.<sup>7</sup> However, immunohistochemical (IHC) analysis of clinical tissues did not show a clear YAP1 subtype and identified a fourth population negative for ASCL1, NEUROD1, and POU2F3.<sup>8</sup> As these studies show, the heterogeneity of SCLC has attracted greater attention in recent years and is expected to be applied to elucidation of drug resistance mechanisms and new molecular targets for treatment.

Personalized precision medicine for SCLC is an urgent unmet need that, thus far, has not progressed mainly because its molecular pathological characteristics are not fully understood. Indeed, although molecular-targeted drugs such as PARP inhibitors, Aurora kinase inhibitors, and BCL2 inhibitors are promising treatments for SCLC, none are currently in clinical use.<sup>9–11</sup> To establish highly accurate precision medicine for patients with SCLC, potential biomarkers to predict the effectiveness of these molecular-targeted agents must be identified. In addition to the aforementioned drugs, the US Food and Drug Administration (FDA) recently approved lurbinectedin as a second-line treatment for SCLC.<sup>12</sup> Although favorable results have been obtained in a large-scale clinical trial with lurbinectedin,<sup>13</sup> SCLC patient cohorts for which the drug will be highly effective remain unknown.

Here, we investigated potential correlations between the expression of four transcription factors driving SCLC (ASCL1, NEUROD1, POU2F3, and YAP1) and sensitivities of therapeutic agents including lurbinectedin in SCLC cell lines. In addition, protein expression of these factors was measured by IHC in a cohort of clinical samples of high-grade neuroendocrine carcinoma (HGNEC), including SCLC and large-cell neuroendocrine carcinoma (LCNEC).

## METHODS

### Cell lines

On the basis of the Cancer Cell Line Encyclopedia and previous reports, we selected four SCLC cell lines with high expression of ASCL1, NEUROD1, POU2F3, or YAP1. In addition, we selected four cell lines expressing a combination of these four factors for a total of eight SCLC cell lines.

All cell lines were purchased from American Type Culture Collection (Manassas, VA). Cell lines were maintained in RPMI-1640 supplemented with 10% fetal bovine serum (FBS) or HITES supplemented with 5% FBS without antibiotics at 37°C in a humidified atmosphere containing 5% CO<sub>2</sub> and 95% air.

### Tumor samples

We retrospectively reviewed 105 patients who underwent surgical treatment at Tottori University Hospital or one its four affiliated hospitals (Tottori Prefectural Central Hospital, Tottori Prefectural Kousei Hospital, Yonago Medical Center, and Matsue Medical Center) and were diagnosed as having primary HGNEC between January 2005 to December 2019. The certified review board of each participating institution approved this retrospective study. We rereviewed the pathological diagnosis of collected tissues based on the 2015 World Health Organization classification.

### RNA extraction and cDNA synthesis

Total RNA was obtained from cell lines using an RNeasy Mini kit (Qiagen). RNA concentrations were measured with a Nanodrop 2000 spectrophotometer (Thermo Fisher Scientific). After RNA extraction, cDNA was generated from 750 ng of total RNA using a high-capacity cDNA reverse transcription kit (Thermo Fisher Scientific).

### Gene expression analysis by quantitative reverse transcription-polymerase chain reaction (qRT-PCR)

mRNA expression levels of ASCL1, NEUROD1, YAP1, and POU2F3 genes were evaluated in cell lines by qRT-PCR with a LightCycler 96 system (Roche Diagnostics) using validated TaqMan primers, TaqMan probes, and TaqMan Gene Expression Master Mix (Thermo Fisher Scientific) according to the manufacturer's protocol. The beta-actin (ACTB) gene was employed as an internal reference gene to normalize input cDNA. Relative gene expression levels were calculated using the standard curve method.

### Western blot analysis

Cells were washed with phosphate-buffered saline and then lysed in radioimmunoprecipitation assay buffer supplemented with protease inhibitor cocktail tablets (cOmplete; Roche Diagnostics) and phosphatase inhibitor tablets (PhosSTOP; Roche Diagnostics). Protein contents were quantified using XL-Bradford (SDS-PAGE Adapted) (Integrale). Lysates (10 µg) were resolved by sodium dodecyl sulfate-polyacrylamide gel electrophoresis (SDS-PAGE) gels and electrotransferred onto

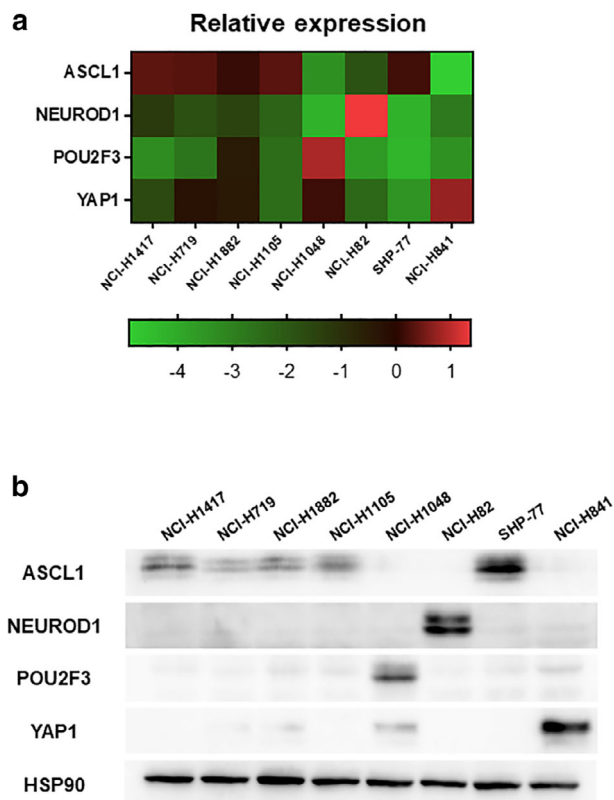


**FIGURE 1** Subtype classification of eight small cell lung cancer (SCLC) cell lines. (a) Comparison of relative mRNA expression levels of ASCL1, NEUROD1, POU2F3, and YAP1 in each cell line. ASCL1 is highly expressed in five cell lines (NCI-H1417, NCI-H719, NCI-H1882, NCI-H1105), NEUROD1 is highly expressed in NCI-H82, POU2F3 in NCI-H1048, and YAP1 in NCI-H841. (b) Protein expression profiles of ASCL1, NEUROD1, POU2F3, and YAP1 in eight SCLC cancer cell lines. Western blots show that SHP-77 highly expresses ASCL1 protein, NCI-H82 highly expresses NEUROD1 protein, NCI-H1048 highly expresses POU2F3 protein, and NCI-H841 highly expresses YAP1 protein

polyvinylidene difluoride membranes (Immobilon; Merck Millipore). After blocking membranes for 90 min at room temperature, they were incubated overnight at 4°C with one of the following primary antibodies (1:1000): rabbit monoclonal anti-ASCL1 (ab211327; Abcam), rabbit monoclonal anti-NEUROD1 (ab109224; Abcam), mouse monoclonal anti-POU2F3 (sc-293 402; Santa Cruz Biotechnology), and rabbit monoclonal anti-YAP1 (14 074; Cell Signaling Technology). Hsp90 levels were used as a control for protein loading. After incubation with primary antibodies, membranes were incubated with a secondary antibody for 1 h at room temperature. Horseradish peroxidase-linked anti-rabbit (Cytiva) and anti-mouse (Cytiva) antibodies were used as secondary antibodies. Proteins were detected by enhanced chemiluminescence (LAS-4000; Cytiva).

### In vitro drug assay

A WST-8 assay was used to analyze the effects of each drug. Numbers of cells per well was determined according to the

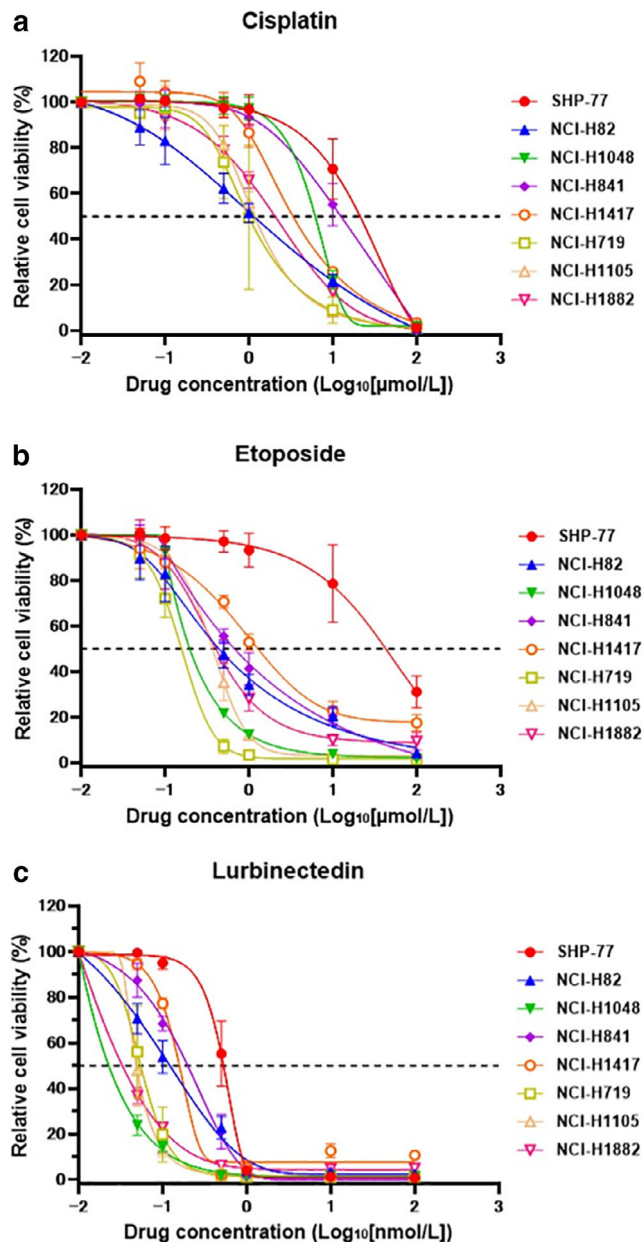


**FIGURE 2** Drug concentration and relative viability of cell lines. Cell lines were cultured in the presence of cisplatin (Fig. 2a), etoposide (Fig. 2b), or lurbinedectin (Fig. 2c) for 72 h and then assayed for cell viability using a WST assay

growth rate of cell lines (NCI-H841:  $1 \times 10^4$  cells per well; SHP-77, NCI-H82, NCI-H1048:  $2 \times 10^4$  cells per well; NCI-H719, NCI-H1105, NCI-H1417, NCI-H1882:  $4 \times 10^4$  cells per well). Cells were cultured in 96-well plates and exposed to seven different concentrations of the drug, including controls. After 72 h of drug administration, cells were processed using cell counting kit-8 (Dojin Chemical) reagents and viability was assessed by measuring the absorbances of each well at 450 nm and 600 nm (reference wavelengths). Etoposide (Tokyo Chemical Industry) and lurbinedectin (MedChemExpress) were dissolved in dimethyl sulfoxide and stored at  $-80^\circ\text{C}$ . Cisplatin (Tokyo Chemical Industry) was dissolved in saline solution at

**TABLE 1** IC<sub>50</sub> values of anticancer drugs in SCLC cell lines

Cell line	Subtype	Cisplatin (μM)	Etoposide (μM)	Lurbinectedin (nM)
NCI-H1417	ASCL1	4.68 (0.83)	1.75 (0.11)	0.154 (0.001)
NCI-H719	ASCL1	1.51 (1.11)	0.15 (0.02)	0.058 (0.015)
NCI-H1882	ASCL1	1.95 (0.28)	0.45 (0.13)	0.042 (0.002)
NCI-H1105	ASCL1	1.20 (0.01)	0.36 (0.07)	0.049 (0.009)
NCI-H1048	POU2F3	6.00 (1.81)	0.30 (0.01)	0.034 (0.002)
NCI-H82	NEUROD1	1.16 (0.33)	0.56 (0.17)	0.124 (0.025)
SHP-77	ASCL1	15.81 (3.15)	44.08 (23.32)	0.520 (0.052)
NCI-H841	YAP1	11.35 (2.52)	0.81 (0.12)	0.177 (0.030)

37°C, stored at 4°C, and used within 2 w. Antiproliferative activity was measured as the 50% growth-inhibitory concentration (IC<sub>50</sub>) for each cell line.

### Immunohistochemical analysis

IHC staining was performed with Histostainer-36A (Nichirei Biosciences). Primary antibodies were as follows: rabbit monoclonal anti-ASCL1 (ab211327, Abcam; 1:250), rabbit monoclonal anti-NEUROD1 (ab213725, Abcam; 1:1000), mouse monoclonal anti-POU2F3 (sc-293 402, Santa Cruz Biotechnology; 1:500), and rabbit monoclonal anti-YAP1 (14 074; Cell Signaling Technology; 1:400). Sections (4 μm thick) were deparaffinized, hydrated, incubated in heat processor solution pH 9 (715 291, Nichirei Biosciences) at 100°C for 40 min, blocked with 3% H<sub>2</sub>O<sub>2</sub> (715 242, Nichirei Biosciences) for 5 min, and incubated primary antibodies for 60 min. Subsequently, slides were incubated with second antibody MAX-PO (R) (724 142; Nichirei Biosciences) or MAX-PO(M) (724 132; Nichirei Biosciences) for 30 min, visualized with DAB (725 191; Nichirei Biosciences), and counterstained with hematoxylin. IHC results were recorded as staining intensity (0, negative; 1, weak; 2, medium; 3, strong) and percentage of positive cells (1%–100%). According to previous studies, we calculated histoscores (H-scores) by multiplying the staining intensity and percentage of positive cells. H-scores were calculated for only the neuroendocrine component if the sample involved combined histology. We classified tumor samples into four transcriptional subtypes: ASCL1, NEUROD1, POU2F3, and YAP1 by their relative predominance of them. If all H-scores were less than 1, the tumor was classified as not otherwise specified (NOS). All slides were evaluated by two of the authors (S.M. and Y.O.) and a qualified pathologist (Y.U.).

### Statistical analysis

All statistical tests were performed using GraphPad Prism 9 (GraphPad Software) and SPSS statistical software version 27 (SPSS). Dose–response curves and IC<sub>50</sub> values were also calculated using GraphPad Prism 9. Spearman's rank correlation coefficient was used to determine correlations between relative mRNA expression of cell lines and sensitivity to

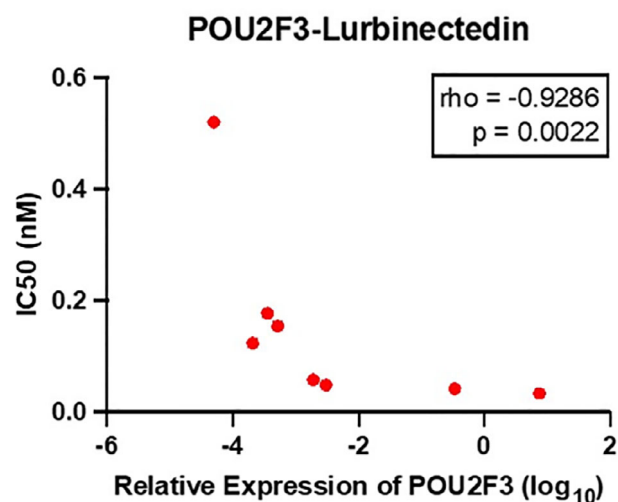


**FIGURE 3** Correlation between relative expression of POU2F3 and IC<sub>50</sub> of lurbinectedin. Spearman's rank correlation coefficient showed a negative correlation between POU2F3 mRNA expression level and the IC<sub>50</sub> value of lurbinectedin ( $\rho = -0.9286$ ,  $p = 0.0022$ ,  $n = 8$ ). IC<sub>50</sub>, half maximal inhibitory concentration

drugs. Chi-square test, Kruskal–Wallis test, and Welch's *t*-test were used to compare clinicopathological factors for each dominant phenotype between groups.

## RESULTS

### Subtype classification of SCLC cell lines

We analyzed the subtype classification of eight SCLC cell lines by qRT-PCR and western blot analysis. qRT-PCR results revealed that ASCL1 was highly expressed in five cell lines (NCI-H1417, NCI-H719, NCI-H1882, NCI-H1105), NEUROD1 was highly expressed in NCI-H82, POU2F3 in NCI-H1048, and YAP1 in NCI-H841 (Figure 1a). Among the three independent experiments, one for NEUROD1 expression in NCI-H1048, one for POU2F3 expression in NCI-H82, and two for POU2F3 expression in SHP-77 were excluded because of low detection sensitivity. Western blots show that SHP-77 had the highest protein expression of ASCL1, NCI-H82 had the highest protein expression of

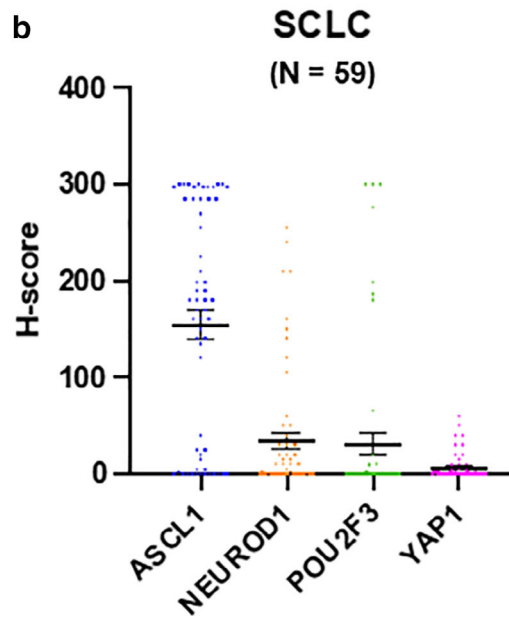
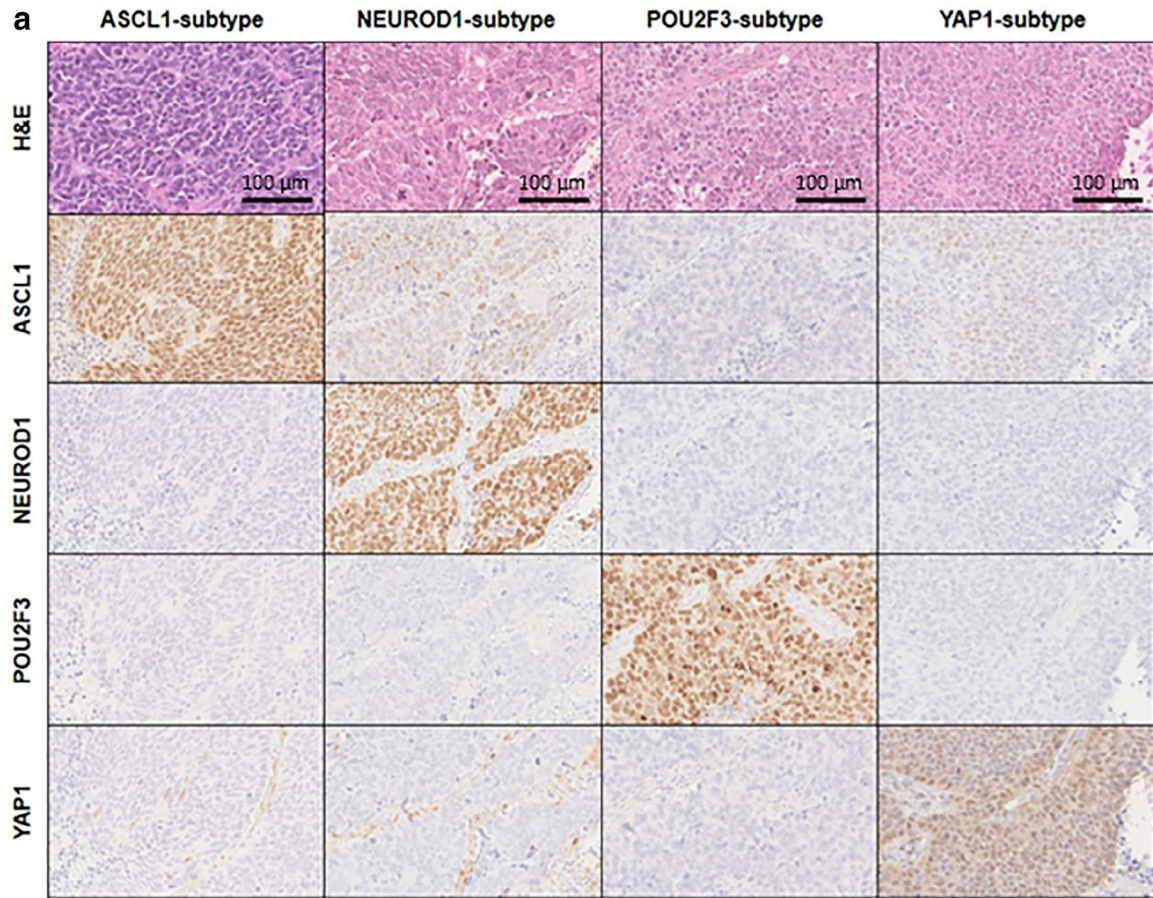


**FIGURE 4** Immunohistochemistry (IHC) expression patterns and score of SCLC. (a) Histological images of SCLC subtypes as defined by expression of ASCL1, NEUROD1, POU2F3, and YAP1 (magnification 40×). The H-score of YAP1 was generally low. (b) Comparison of H-score in SCLC. The H-score for ASCL1 was high overall, followed by NEUROD1. Most of the POU2F3 positive cases had H-scores distributed around 200 and 300 as the entire tumor was positive. The H-score of YAP1 was generally low. The bars show the mean and SEM. H-score: histoscore, calculated by multiplying the staining intensity and percentage of positive cells

TABLE 2 Clinicopathological characteristics of patients

Characteristic	Subtypes						p-value
	All patients (N = 59)	ASCL1 (N = 36)	NEUROD1 (N = 9)	POU2F3 (N = 8)	YAPI (N = 3)	NOS (N = 3)	
Age	72 (66–78)	72 (66–77)	71 (62–80)	73 (70–79)	80	66	0.399
Sex							
Male	51 (86)	32 (89)	8 (89)	6 (75)	2 (67)	3 (100)	0.628
Female	8 (14)	4 (11)	1 (11)	2 (25)	1 (33)	0 (0)	
Smoking pack-years	49 (40–63)	50 (40–73)	50 (39–79)	39 (26–49)	40	40	0.151
Pro-GRP (pg/ml)	75.2 (45.2–141.3)	83.3 (46.6–169.4)	59.3 (46.1–92.4)	67.9 (35.7–143.8)	18.7	88.5	0.367
Surgery							
Lobectomy or greater	30 (51)	18 (50)	5 (56)	6 (75)	1 (33)	0 (0)	0.108
Sublobar resection	25 (42)	17 (47)	4 (44)	1 (13)	1 (33)	2 (67)	
Biopsy	4 (7)	1 (3)	0 (0)	1 (13)	1 (33)	1 (33)	
Curability							
R0	42 (71)	27 (75)	5 (56)	7 (88)	1 (33)	2 (67)	0.221
R1	9 (15)	7 (19)	2 (22)	0 (0)	0 (0)	0 (0)	
R2	8 (14)	2 (6)	2 (22)	1 (13)	2 (67)	1 (33)	
Adjuvant chemotherapy <sup>a</sup>							
Yes	32 (54)	21 (58)	4 (44)	6 (75)	0 (0)	1 (33)	0.304
No	17 (29)	11 (31)	3 (33)	1 (13)	1 (33)	1 (33)	
Not applicable	10 (17)	4 (11)	2 (22)	1 (13)	2 (67)	1 (33)	
Chemotherapy							
Yes	42 (71)	25 (69)	6 (67)	7 (88)	2 (67)	2 (67)	0.871
No	17 (29)	11 (31)	3 (33)	1 (13)	1 (33)	1 (33)	
pT factor							
T1a	1 (2)	0 (0)	0 (0)	0 (0)	0 (0)	1 (33)	0.036
T1b	17 (29)	12 (33)	1 (11)	0 (0)	2 (67)	2 (67)	
T1c	11 (19)	6 (17)	2 (22)	3 (38)	0 (0)	0 (0)	
T2a	23 (39)	16 (44)	4 (44)	3 (38)	0 (0)	0 (0)	
T2b	2 (3)	1 (3)	1 (1)	0 (0)	0 (0)	0 (0)	
T3	4 (7)	1 (3)	1 (1)	1 (13)	1 (33)	0 (0)	
T4	1 (2)	0 (0)	0 (0)	1 (13)	0 (0)	0 (0)	
pN factor							
N0	26 (44)	15 (42)	5 (56)	6 (75)	0 (0)	0 (0)	0.096
N1	6 (10)	5 (14)	1 (11)	0 (0)	0 (0)	0 (0)	
N2	8 (14)	3 (8)	2 (22)	0 (0)	2 (67)	1 (33)	
NX	19 (32)	13 (36)	1 (11)	2 (25)	1 (33)	2 (67)	
Pathological stage							
I	37 (63)	25 (69)	4 (44)	5 (63)	1 (33)	2 (67)	0.356
II	10 (17)	6 (17)	2 (22)	2 (25)	0 (0)	0 (0)	
III	8 (14)	3 (8)	2 (22)	1 (13)	1 (33)	1 (33)	
IV	4 (7)	2 (6)	1 (11)	0 (0)	1 (33)	0 (0)	
Histological subtype							
SCLC	46 (78)	28 (78)	6 (67)	7 (88)	2 (67)	3 (100)	0.706
Combined SCLC	13 (22)	8 (22)	3 (33)	1 (13)	1 (33)	0 (0)	
Lymphatic invasion							
Present	36 (61)	24 (67)	4 (44)	5 (63)	1 (33)	2 (67)	0.659
Absent	19 (32)	10 (28)	4 (44)	3 (38)	1 (33)	1 (33)	
Not applicable	4 (7)	2 (6)	1 (11)	0 (0)	1 (33)	0 (0)	

(Continues)

TABLE 2 (Continued)

	All patients (N = 59)	Subtypes					p-value
		ASCL1 (N = 36)	NEUROD1 (N = 9)	POU2F3 (N = 8)	YAP1 (N = 3)	NOS (N = 3)	
Vascular invasion							
Present	33 (56)	20 (56)	5 (56)	5 (63)	1 (33)	2 (67)	0.791
Absent	22 (37)	14 (39)	3 (33)	3 (38)	1 (33)	1 (33)	
Not applicable	4 (7)	2 (6)	1 (11)	0 (0)	1 (33)	0 (0)	
Pleural invasion							
Present	23 (39)	16 (44)	5 (56)	2 (25)	0 (0)	0 (0)	0.079
Absent	34 (58)	19 (53)	4 (44)	6 (75)	2 (67)	3 (100)	
Not applicable	2 (3)	1 (3)	0 (0)	0 (0)	1 (33)	0 (0)	

Note: Data are shown as number (% among each subtype) or median (25–75 percentile).

Abbreviations: NOS, not otherwise specified; SCLC, small cell lung carcinoma.

<sup>a</sup>Patients who received two or more courses of adjuvant platinum-based chemotherapy.

NEUROD1, NCI-H1048 had the highest protein expression of POU2F3, and NCI-H841 has the highest protein expression of YAP1 (Figure 1b). On the basis of the results of our qRT-PCR and western blot analyses, we classified NCI-H1417, NCI-H719, NCI-H1882, and NCI-H1105 as ASCL1 subtype; NCI-H82 as NEUROD1 subtype; NCI-H1048 as POU2F3 subtype; and NCI-H841 as YAP1 subtype.

### Subtype classification and drug sensitivity

Dose–response curves of cisplatin, etoposide, and lurbinectedin for viability of each SCLC cell line are shown in Figures 2a–c. IC<sub>50</sub> values for these anticancer drugs in the eight SCLC cell lines revealed no association between subtype classification and IC<sub>50</sub> (Table 1).

### Correlation between mRNA expression levels and IC<sub>50</sub> value

We next examined potential correlations between relative mRNA expression of each gene and the IC<sub>50</sub> of each drug. mRNA expression of POU2F3 was weakly correlated with the drug sensitivity of etoposide ( $\rho = -0.7381$ ,  $p = 0.0458$ ) and strongly associated with the drug sensitivity of lurbinectedin ( $\rho = -0.9286$ ,  $p = 0.0022$ ) (Figure S1 and Figure 3). For the relationship between POU2F3 mRNA expression and etoposide drug sensitivity, the result for SHP-77 was a significant outlier; when SHP-77 was excluded, the correlation disappeared ( $\rho = -0.6071$ ,  $p = 0.1667$ ).

### Validation of subtype classification in resected tumors

To evaluate the link between our experimental results and clinical practice, we investigated the frequency of each subtype and clinicopathological factors in high-grade neuroendocrine

carcinoma of the lung. Histological images of SCLC subtypes defined by expression of ASCL1, NEUROD1, POU2F3, and YAP1 (Figure 4a) and LCNEC subtypes (Figure S2A) are shown. Although the staining intensity of LCNEC tended to be weaker than that of SCLC, they could be classified into the same four subtypes identified for SCLC.

The H-score of ASCL1 was generally the highest, followed by NEUROD1. H-scores for most POU2F3-positive cases were distributed around 200 or 300 because the entire tumor was positive. H-score for YAP1 was generally low, with a maximum value of 60 (Figure 4b and Figure S2B). Clinicopathological characteristics of SCLC patients are shown in Table 2. Comparison between phenotypes in SCLC showed significantly smaller tumor size in NOS, but no significant differences in other clinicopathological factors (Table 2). Comparison in HGNEC showed no significant difference in clinicopathological features (Table S1).

### DISCUSSION

Lurbinectedin is a synthetic analog of trabectedin, a small molecule obtained by purifying extracts from the ascidian *Ecteinascidia turbinata*. Lurbinectedin exerts its antitumor effects by (i) inhibiting the cell cycle through DNA adducts, such as the formation of double-strand breaks; (ii) inhibiting RNA polymerase; and (iii) effects on the tumor inflammatory microenvironment.<sup>14–16</sup> A single-arm, open-label, phase II basket study of lurbinectedin 3.2 mg/m<sup>2</sup> every 21 days as a second-line treatment for patients with recurrent SCLC resulted in its approval by the FDA as a second-line treatment option for patients with ES-SCLC due to its high efficacy and acceptable adverse events.<sup>12,13</sup> In this phase II trial, patients with platinum-sensitive tumors had a higher overall response rate to lurbinectedin compared with patients who had platinum-resistant tumors, but no other biomarkers were found to be predictive. In our study, we analyzed the expression of four transcription factors in eight SCLC cell lines, and investigated their sensitivity to cisplatin and etoposide (the standard regimen for

SCLC) and lurbinectedin (a novel therapeutic agent). Most cell lines were highly sensitive to lurbinectedin, while sensitivities to cisplatin and etoposide varied. Although “subtype switching” from high to low ASCL1 expression is a known mechanism of drug resistance in SCLC changes,<sup>7,17,18</sup> trends observed for the cell lines used in this study did not suggest drug resistance. Our findings did reveal a correlation between POU2F3 mRNA expression and the effect of lurbinectedin.

POU2F3 (also known as POU class 2 homeobox 3) is expressed in tuft cells, which are rare chemosensory cells in the airway epithelium.<sup>19</sup> CRISPR screening focused on human transcription factor domains showed that POU2F3 is essential for several SCLC cell lines. Furthermore, cell lines expressing POU2F3 expressed low levels of ASCL1 and NEUROD1.<sup>20</sup> Gay et al. reported that the POU2F3 subtype had the second-highest sensitivity to immune checkpoint inhibitors after “SCLC-Inflamed,” but a worse prognosis.<sup>17</sup> In addition, they evaluated the efficacy of PARP inhibitors and antimetabolites against the POU2F3 subtype.<sup>17</sup> In contrast, there are no known predictors of the effectiveness of lurbinectedin, which is currently available in clinical practice. If lurbinectedin is effective against the POU2F3 subtype in actual clinical practice, as suggested by the results of our study, it would be a significant step for personalized treatment of SCLC. Lurbinectedin also reportedly exerts a synergistic effect with immune checkpoint inhibitors<sup>21</sup> and is expected to be applied clinically as a combination therapy in the future.

To validate the subtype classification method used in our *in vitro* study, we also examined resected HGNEC specimens. Importantly, the use of resected specimens for evaluation allowed us to more accurately assess heterogeneity within a single tumor than biopsy tissue or tissue microarrays. Because samples were obtained from subjects with primarily early-stage cases, we were concerned that the results might be biased. However, calculated H-scores and subtype ratios were generally consistent with those reported by Baine et al.<sup>8</sup> As in previous studies, we found that the H-score of YAP1 was generally low, making it unclear whether it could be considered a subtype.<sup>8</sup> The ability to classify SCLC by IHC staining is helpful for precision medicine in future clinical practice<sup>9–11</sup> and it is noteworthy that LCNEC could be subtyped in the same way as SCLC. Indeed, it is sometimes challenging to distinguish SCLC from LCNEC morphologically,<sup>22</sup> and there is much overlap in gene and protein expression.<sup>23</sup> Although a previous report indicated no apparent difference in treatment efficacy of the SCLC regimen between SCLC and LCNEC,<sup>24</sup> another study reported that the effectiveness of chemotherapy was stratified by the presence or absence of *RB1* gene expression in LCNEC.<sup>25</sup> Although there were no noticeable clinicopathological differences between these subtypes, it will be interesting to see if they have any clinical significance for HGNEC as a therapeutic target.

The next goal in SCLC care is to understand SCLC heterogeneity based on resected tissue, circulating tumor cells, and circulating tumor DNA to address individualized treatment and drug resistance mechanisms for each subtype.

Based on our findings, it will be advantageous to investigate whether lurbinectedin affects the POU2F3 subtype in a clinical setting.

## ACKNOWLEDGMENTS

This work was supported by Grants-in-Aid for Scientific Research from the Japan Society for the Promotion of Science (JSPS KAKENHI grant no. JP 19K18215). We thank Edanz (<https://jp.edanz.com/ac>) for editing a draft of this manuscript.

## CONFLICT OF INTEREST

No authors report any conflict of interest.

## ORCID

Tomohiro Haruki  <https://orcid.org/0000-0002-6070-3926>

## REFERENCES

- Howlander N, Forjaz G, Mooradian MJ, Meza R, Kong CY, Cronin KA, et al. The effect of advances in lung-cancer treatment on population mortality. *N Engl J Med*. 2020;383(7):640–9.
- Liu SV, Reck M, Mansfield AS, Mok T, Scherpereel A, Reinmuth N, et al. Updated overall survival and PD-L1 subgroup analysis of patients with extensive-stage small-cell lung cancer treated with Atezolizumab, carboplatin, and etoposide (IMpower133). *J Clin Oncol*. 2021;39(6):619–30.
- Goldman JW, Dvorkin M, Chen Y, Reinmuth N, Hotta K, Trukhin D, et al. Durvalumab, with or without tremelimumab, plus platinum-etoposide versus platinum-etoposide alone in first-line treatment of extensive-stage small-cell lung cancer (CASPIAN): updated results from a randomised, controlled, open-label, phase 3 trial. *Lancet Oncol*. 2021;22(1):51–65.
- Rudin CM, Poirier JT. Small-cell lung cancer in 2016: shining light on novel targets and therapies. *Nat Rev Clin Oncol*. 2017;14(2):75–6.
- George J, Lim JS, Jang SJ, Cun Y, Ozretić L, Kong G, et al. Comprehensive genomic profiles of small cell lung cancer. *Nature*. 2015;524(7563):47–53.
- Rudin CM, Poirier JT, Byers LA, Dive C, Dowlati A, George J, et al. Molecular subtypes of small cell lung cancer: a synthesis of human and mouse model data. *Nat Rev Cancer*. 2019;19(5):289–97.
- Ireland AS, Micinski AM, Kastner DW, Guo B, Wait SJ, Spainhower KB, et al. MYC drives temporal evolution of small cell lung cancer subtypes by reprogramming neuroendocrine fate. *Cancer Cell*. 2020;38(1):60–78.e12.
- Baine MK, Hsieh MS, Lai WV, Egger JV, Jungbluth AA, Daneshbod Y, et al. SCLC subtypes defined by ASCL1, NEUROD1, POU2F3, and YAP1: a comprehensive Immunohistochemical and histopathologic characterization. *J Thorac Oncol*. 2020;15(12):1823–35.
- Poirier JT, George J, Owonikoko TK, Berns A, Brambilla E, Byers LA, et al. New approaches to SCLC therapy: from the laboratory to the clinic. *J Thorac Oncol*. 2020;15(4):520–40.
- Mak DWS, Li S, Minchom A. Challenging the recalcitrant disease-developing molecularly driven treatments for small cell lung cancer. *Eur J Cancer*. 2019;119:132–50.
- Frese KK, Simpson KL, Dive C. Small cell lung cancer enters the era of precision medicine. *Cancer Cell*. 2021;39(3):297–9.
- Singh S, Jaigirdar AA, Mulkey F, Cheng J, Hamed SS, Li Y, et al. FDA approval summary: lurbinectedin for the treatment of metastatic small cell lung cancer. *Clin Cancer Res*. 2021;27(9):2378–82.
- Trigo J, Subbiah V, Besse B, Moreno V, López R, Sala MA, et al. Lurbinectedin as second-line treatment for patients with small-cell lung cancer: a single-arm, open-label, phase 2 basket trial. *Lancet Oncol*. 2020;21(5):645–54.
- Leal JF, Martínez-Díez M, García-Hernández V, Moneo V, Domingo A, Bueren-Calabuig JA, et al. PM01183, a new DNA minor



- groove covalent binder with potent in vitro and in vivo anti-tumour activity. *Br J Pharmacol*. 2010;161(5):1099–110.
15. Santamaria Nuñez G, Robles CM, Giraudon C, Martínez-Leal JF, Compe E, Coin F, et al. Lurbinectedin specifically triggers the degradation of phosphorylated RNA polymerase II and the formation of DNA breaks in cancer cells. *Mol Cancer Ther*. 2016;15(10):2399–412.
  16. Belgiovine C, Bello E, Liguori M, Craparotta I, Mannarino L, Paracchini L, et al. Lurbinectedin reduces tumour-associated macrophages and the inflammatory tumour microenvironment in preclinical models. *Br J Cancer*. 2017;117(5):628–38.
  17. Gay CM, Stewart CA, Park EM, Diao L, Groves SM, Heeke S, et al. Patterns of transcription factor programs and immune pathway activation define four major subtypes of SCLC with distinct therapeutic vulnerabilities. *Cancer Cell*. 2021;39(3):346–360.e7.
  18. Stewart CA, Gay CM, Xi Y, Sivajothi S, Sivakamasundari V, Fujimoto J, et al. Single-cell analyses reveal increased intratumoral heterogeneity after the onset of therapy resistance in small-cell lung cancer. *Nat Cancer*. 2020;1:423–36.
  19. Yamashita J, Ohmoto M, Yamaguchi T, Matsumoto I, Hirota J. *Skn-1a/Pou2f3* functions as a master regulator to generate *Trpm5*-expressing chemosensory cells in mice. *PLoS One*. 2017;12(12):e0189340.
  20. Huang YH, Klingbeil O, He XY, Wu XS, Arun G, Lu B, et al. *POU2F3* is a master regulator of a tuft cell-like variant of small cell lung cancer. *Genes Dev*. 2018;32(13–14):915–28.
  21. Xie W, Forveille S, Iribarren K, Sauvat A, Senovilla L, Wang Y, et al. Lurbinectedin synergizes with immune checkpoint blockade to generate anticancer immunity. *Oncotargets Ther*. 2019;8(11):e1656502.
  22. den Bakker MA, Willemsen S, Grünberg K, Noorduijn LA, van Oosterhout MFM, van Suylen RJ, et al. Small cell carcinoma of the lung and large cell neuroendocrine carcinoma interobserver variability. *Histopathology*. 2010;56(3):356–63.
  23. George J, Walter V, Peifer M, Alexandrov LB, Seidel D, Leenders F, et al. Integrative genomic profiling of large-cell neuroendocrine carcinomas reveals distinct subtypes of high-grade neuroendocrine lung tumors. *Nat Commun*. 2018;9(1):1048.
  24. Kenmotsu H, Niho S, Tsuboi M, Wakabayashi M, Ishii G, Nakagawa K, et al. Randomized phase III study of irinotecan plus cisplatin versus etoposide plus cisplatin for completely resected high-grade neuroendocrine carcinoma of the lung: JCOG1205/1206. *J Clin Oncol*. 2020;38(36):4292–301.
  25. Derks JL, Leblay N, Thunnissen E, van Suylen R, den Bakker MA, Groen HJM, et al. Molecular subtypes of pulmonary large-cell neuroendocrine carcinoma predict chemotherapy treatment outcome. *Clin Cancer Res*. 2018;24(1):33–42.

## SUPPORTING INFORMATION

Additional supporting information may be found in the online version of the article at the publisher's website.

**How to cite this article:** Matsui S, Haruki T, Oshima Y, Kidokoro Y, Sakabe T, Umekita Y, et al. High mRNA expression of *POU2F3* in small cell lung cancer cell lines predicts the effect of lurbinectedin. *Thorac Cancer*. 2022;13:1184–92. <https://doi.org/10.1111/1759-7714.14382>